Proc. Lunar Sci. Conf. 6th (1975), p. 2571–2583.
Printed in the United States of America

Lunar crater chains of non-impact origin

DEAN EPPLER*
Lunar Science Institute, 3303 NASA Road 1, Houston, Texas 77058

GRANT HEIKEN
Los Alamos Scientific Laboratories, Los Alamos, New Mexico 87544

Abstract—Lunar crater chains consisting of three or more aligned craters with similar states of degradation were identified from Apollo 15, 16, and 17 orbital photographs and selected for detailed study. Secondary crater chains were separated from those of non-impact origin using morphologic criteria and areal association with large impact craters. Three possible modes of origin were determined: collapsed lava tubes (group 1), cinder cones (group 2), and highland volcanoes (group 3). Crater chains which were too subdued to permit determination or origin were placed in group 4. Crater chains from mare regions range from 20 to 40 km long and appear to have no preferred structural control of their orientation. The mode of origin for mare crater chains appears to be either group 1 or group 2. Highland crater chains range from 1 to 113 km long and may be structurally controlled by the lunar grid system with orientations at 45°, 330°, and 360°. The crater chains for which origin can be determined are in group 3. Theoretical viscosities calculated for returned highland samples indicate that the viscosity at 1000°C of these rocks is similar to measured viscosities of Hawaiian basalts. This may infer that highland volcanic crater chains were originally similar in form to groups 1 and 2.

INTRODUCTION

CRATER CHAINS forming linear and sinuous patterns are found on both mare and highland surfaces, and their distribution patterns and mode of origin have been the subject of much research. Many authors have used crater chains to support both the volcanic and meteorite impact origin of lunar craters. Early arguments for both origins have been reviewed by Shoemaker (1962) and Mutch (1971).

Photogeologic studies of non-random linear arrays of craters have been conducted by Fielder and Marcus (1967), Fielder (1968), Shemyakin (1969), and Elston *et al.* (1971). These studies have been concerned with preferential alignments of craters over the entire surface of the moon. Studies of crater morphology and ejecta patterns, and morphologic relations between individual craters within a given chain have been conducted by El-Baz (1969), Scott *et al.* (1971), and Oberbeck and Morrison (1973). Study of a specific chain combining aspects of both these methods has been conducted by Eppler and Heiken (1974).

Crater chains have been interpreted as endogenetic (Schumm, 1970; Shoemaker, 1962), collapsed lava tubes (Greeley, 1971a,b; Greeley and Hyde, 1971; Cruikshank and Wood, 1973), or as secondary craters (Guest and Murray, 1971; Oberbeck, 1971; and Oberbeck and Morrison, 1973).

*Present address: Department of Geology, University of New Mexico, Albuquerque, New Mexico 87131.

DESCRIPTION OF STUDY

Panoramic and metric mapping camera photographs from Apollos 15, 16, and 17 were used in this study. The photography was used to determine the location, trend and length, geologic setting, dimensions of individual craters, and relative state of degradation of each chain. Subjective measurement of crater degradation was based on the techniques of Pohn and Offield (1970). A simple geologic map was constructed when possible, but in most cases, the degraded state of the individual craters allowed construction of only the simplest geomorphic outline. Crater chains selected for the study consisted of three or more aligned craters with the same or similar state of degradation.

Chains of secondary impact craters were excluded from the study for a number of reasons. A considerable amount of research has been reported in the literature so that the mechanisms of formation and the morphology of the resulting chain are well known. Possible secondary crater chains were identified and excluded from the study using the following criteria: (1) Ridges of ejecta extending a significant distance away from the chain in any orientation with the chain axis, from perpendicular to low-angle V-shaped; Oberbeck and Morrison (1973) have established this criterion theoretically, experimentally, and by careful study of orbital photographs. (2) Chains associated with clusters or fields of secondary craters, such as those seen around Copernicus. (3) Orientation of a subdued crater chain radial to a large impact of similar degradation. These criteria were quite subjective in many cases. Readers desiring further information on secondary crater chains are referred to the work of Guest and Murray (1971), Oberbeck (1971), and Oberbeck and Morrison (1973).

Most of the crater chains studied have been severely degraded by later impacts and mass-wasting. These features masked any structure visible in the crater walls, as well as extensively altering crater morphology. Ejecta patterns are also greatly subdued. Consequently, determination of origin based on these characteristics was difficult or impossible.

Crater chains separated from secondary chains were examined in stereo photography and separated into three possible genetic groups: collapsed lava tubes (group 1), lines of cinder cones (group 2), and highland volcanoes (group 3). Chains which were too subdued to permit determination of origin were placed in group 4. Group 1 and 2 chains are primarily confined to mare areas, and group 3 is confined to the highland areas.

GENERAL FEATURES OF MARE CRATER CHAINS

Most of the crater chains studied were less than 2 km wide and 20–40 km long. Crater degradation fell within categories 4–5 of Pohn and Offield (1970) for most of the craters studied. There appears to be no preferred orientation or structural control of mare crater chains (Fig. 1), but care must be taken in interpreting these results because of the low number of measurements (23). Of the mare crater chains identified, eighteen are in group 1, one is in group 2, and four are in group 4.

Table 1. Crater chains identified from Apollo photography.
M = mare H = highland N = nearside F = farside HO = high oblique

Location[ab]		Trend[a]	Photo numbers[c]	Genetic group	Geologic setting	Length[d]
1.5°N	49.5°E	236	AS15-0124 + 0129	1	NM	7.0
28.5°N	43.0°W	38	AS15-0314 + 0319	1	NM	16.9
22.0°N	4.5°W	43	AS15-0206 + 0211	1	NM	10.8
18.5°S	115.0°E	15	AS15-9631 + 9636	4	NH	48.6
25.0°N	2.0°W	310	AS15-9926	4	NM	10.4
25.0°N	2.0°W	270	AS15-9926	4	NM	7.1
16.5°N	22.0°E	360	AS15-9886 + 9891	1	NM	H0
13.0°N	65.5°E	300	AS15-9184 + 9189	1	NM	11.2
12.3°S	4.4°W	10	AS16-0715 + 0716	4	NM	2.0
3.8°S	43.6°E	42	AS16-0811 + 0812	1	NM	HO
9.4°S	13.3°W	304	AS16-1683 + 1684	4	NM	8.4
23.1°N	10.5°E	282	AS17-0952 + 0953	1	NM	1.4
19.7°N	29.9°E	337	AS17-2285 + 2290	1	NM	2.1
19.9°S	27.5°E	358	AS17-2317 + 2322	1	NM	23.8
15.1°N	52.5°E	333	AS17-2684 + 2689	1	NM	4.6
13.6°N	33.6°E	81	AS17-3005 + 3010	1	NM	3.7
11.2°N	41.1°E	314	AS17-2981 + 2986	1	NM	5.9
13.2°N	35.0°E	315	AS17-3001 + 3006	1	NM	7.8
22.8°N	9.1°W	81	AS17-3043 + 3048	1	NM	12.9
23.0°N	17.8°W	360	AS17-3069 + 3074	1	NM	6.8
23.1°N	29.8°W	45	AS17-3107	1	NM	11.6
22.6°N	36.7°W	337	AS17-3126	1	NM	4.2
19.9°S	27.5°E	288	AS17-2317 + 2322	2	NM	10.4
16.8°N	63.3°E	288	AS17-2321 + 2326	1	NM	7.5
23.5°S	168.0°E	308	AS15-8860 + 8865	4	FH	1.3
23.5°N	9.5°W	270	AS15-0220 + 0225	4	NH	20.7
21.0°N	2.0°W	270	AS15-0198 + 0203	1	FH	10.7
13.5°S	123.5°E	360	AS15-8997 + 9002	4	NH	4.4
19.0°S	139.0°W	50	AS15-8945 + 8950	4	FH	17.4
8.5°S	90.5°E	325	AS15-9719 + 9724	4	NH	8.6
19.5°S	91.0°E	340	AS15-9998 + 0003	4	FH	62.5
26.0°N	4.5°W	314	AS15-9394 + 9399	4	NH	6.6
5.7°N	138.8°E	20	AS16-0062 + 0063	3	FH	113.0
8.2°N	163.2°E	32	AS16-0041 + 0042	4	FH	38.2
9.0°S	9.0°E	68	AS16-0445 + 0446	4	FH	7.9
9.3°S	3.7°E	18	AS16-0575 + 0576	4	NH	103.6
8.6°S	59.3°E	16	AS16-0668 + 0669	4	NH	HO
5.8°S	17.7°E	8	AS16-0829 + 0830	4	NH	HO
8.4°N	156.2°E	333	AS16-0863 + 0864	4	FH	15.8
9.2°S	6.0°E	340	AS16-0982 + 0983	4	NH	161.5
6.7°N	123.4°E	272	AS16-1577 + 1578	4	FH	7.5
9.1°N	121.7°E	48	AS16-2706 + 2707	4	FH	26.7
11.6°S	144.4°E	331	AS17-0700 + 0701	4	FH	15.8
7.0°S	130.0°E	360	AS17-0713 + 0714	3	FH	10.9
10.8°S	162.9°E	293	AS17-1722 + 1727	4	FH	38.4
9.3°S	158.2°E	360	AS17-1738 + 1743	4	FH	5.7
9.2°S	146.3°E	45	AS17-1989 + 1994	4	FH	124.0

Table 1. (*Continued*).

Location[ab]	trend[a]	Photo numbers[c]	Genetic group	Geologic setting	Length[d]
8.5°S 134.1°E	45	AS17-1995 + 2000	4	FH	13.7
5.0°S 134.1°E	337	AS17-2023 + 2028	4	FH	32.8
17.5°S 127.3°E	45	AS17-2776	4	FH	38.5
20.3°N 32.9°E	45	AS17-2744 + 2749	4	NH	9.8
3.8°N 59.9°E	360	AS17-2919 + 2924	4	NH	7.3
14.4°S 130.2°E	270	AS17-1479 + 1480	4	FH	HO

[a]In degrees.
[b]Principal point of first photo number, data from mapping camera and panoramic camera indices for Apollos 15, 16, and 17.
[c]Stereo pairs.
[d]In kilometers.

Group 1: *Examples of collapsed lava tubes*

The chain is located south of the crater Diophantus on the western rim of Mare Imbrium (22.6°N, 36.7°W) and consists of five rimless, round to irregular craters separated from a large, rimless doublet of the same origin (Fig. 2). The craters are bowl-shaped to irregular and appear to be mantled with a fine regolith. Incipient slumps are well developed, particularly around the large doublet. No blocks are visible on the floors, or layering or structure in the walls. The chain is 4.2 km long, and the large doublet is 2.6 km wide. Regionally, the chain is associated with a set of the Imbrium rilles, and is 60 km northwest of Euler β, which was mapped by

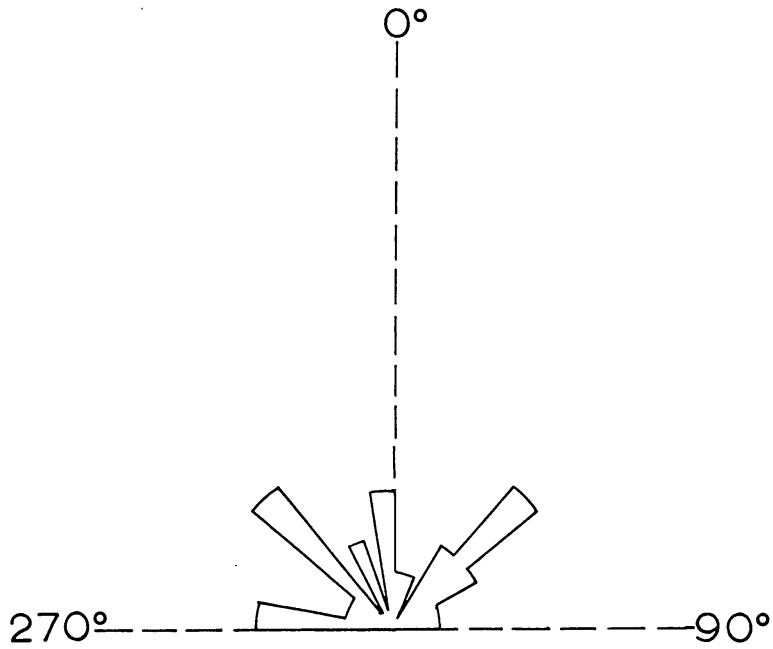

Fig. 1. Pie diagram of the axial trends of mare crater chains. Measurement interval is 10°. Total of 23 measurements.

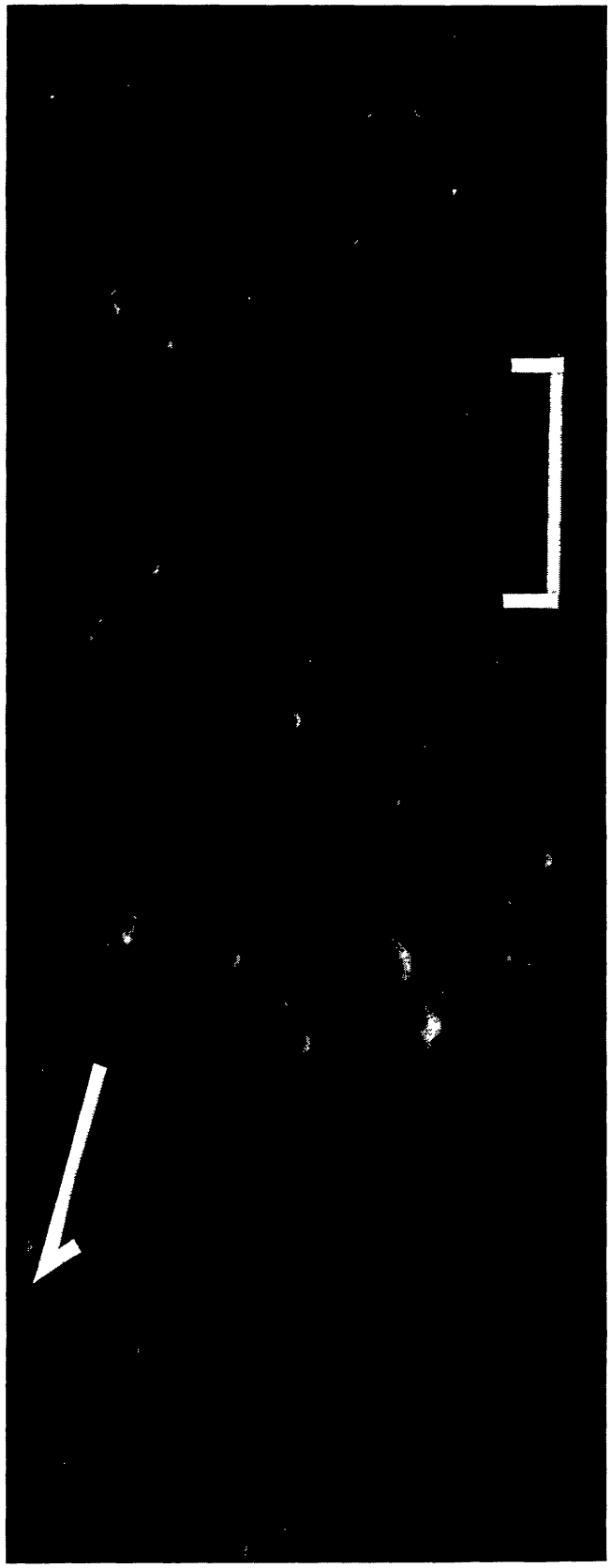

Fig. 2. Genetic type 1 crater chain south of crater Diophantus (22.6°N, 36.7°W). A chain of small collapse craters is separated from 2 larger craters with the same origin. Note the group of secondary craters south and east of the large doublet. Scale bar is 5 km. Arrow points north. NASA Photo AS17-3126.

Schaber (1973) as the source of Eratosthenian mare lavas. The Diophantus chain is on the western edge of an area mapped tentatively as earliest (I) to middle (II) age Eratosthenian lavas.

Terrestrial lava tube formation has been investigated extensively by several authors as an analog to a variety of lunar features. This research involved study of collapsed and partly collapsed lava tubes and field investigations of fluid behavior of active lava flows.

Ollier and Brown (1965), Greeley (1971a,b), and Greeley and Hyde (1971) have established the following criteria for lava tube formation: (1) Low-viscosity lava (pahoehoe to fluid aa) and low velocity of the moving flow. Greeley (1971a) has reported that the development of turbulent flow will result in the development of open channels rather than lava tubes. Specific limiting velocities and viscosities are not known. (2) Thin flows so as to non-uniform fluid velocities within the basalt. Slower moving regions of the flow would solidify first, allowing the formation of a conduit through which fluid would continue to flow.

The mode of formation of terrestrial lava tubes, as established by Greeley (1971a), involves continued flow of lava beneath a solidified surface crust. As the flow cools, fluid lava becomes restricted into a pipe-like conduit. When the supply of lava from the vent is exhausted, the conduit may drain beneath the crust to form a void which becomes a lava tube. Collapse of the roof of a tube may be caused by either withdrawal of support of the roof by draining the conduit before the overlying crust was sufficiently thick to support its own weight, or by failure of the roof during bedrock shaking caused by meteorite impact or tectonic activity.

Absence of roof blocks on the floors of group 1 crater chains argues against the lava tube hypothesis. However, theoretical studies of lunar micrometeorite erosion rates by Hörz *et al.* (1974, personal communication) indicate that sufficient time has elapsed since the emplacement of the youngest Mare Imbrium lavas to break down these blocks. The extreme size contrast between group 1 crater chains and terrestrial lava tubes also argues against this mode of origin, but work by Howard and others (1972) on Hadley Rille indicates the feasibility of large lunar lava tubes of the magnitude required to produce some group 1 crater chains.

Group 2: Examples of lunar cinder cones

The chain is located southwest of the Apollo 17 landing site in Mare Serenitatis (19.9°S, 27.5°E), and consists of two conical mounds at either end, each with a central crater, and a number of small, rimless pits in between the cones (Fig. 3). This feature has also been described by Scott (1974) and Bryan and Adams (1974). The mounds are located at either end of a line of small, rimless craters and hummocks. The chain follows the crest of a slight upwarp in the mare surface. Regolith appears to mantle the terrain in patches around the chain, and the two cones appear to be made of fine-grained debris. Lobate masses of material on the lower slopes of the southern cone appear to be mass-wasted regolith, supporting this observation. The southern cone is slightly breached, and the northern cone is completely breached. Two straight rilles coalesce beneath the southern cone, and

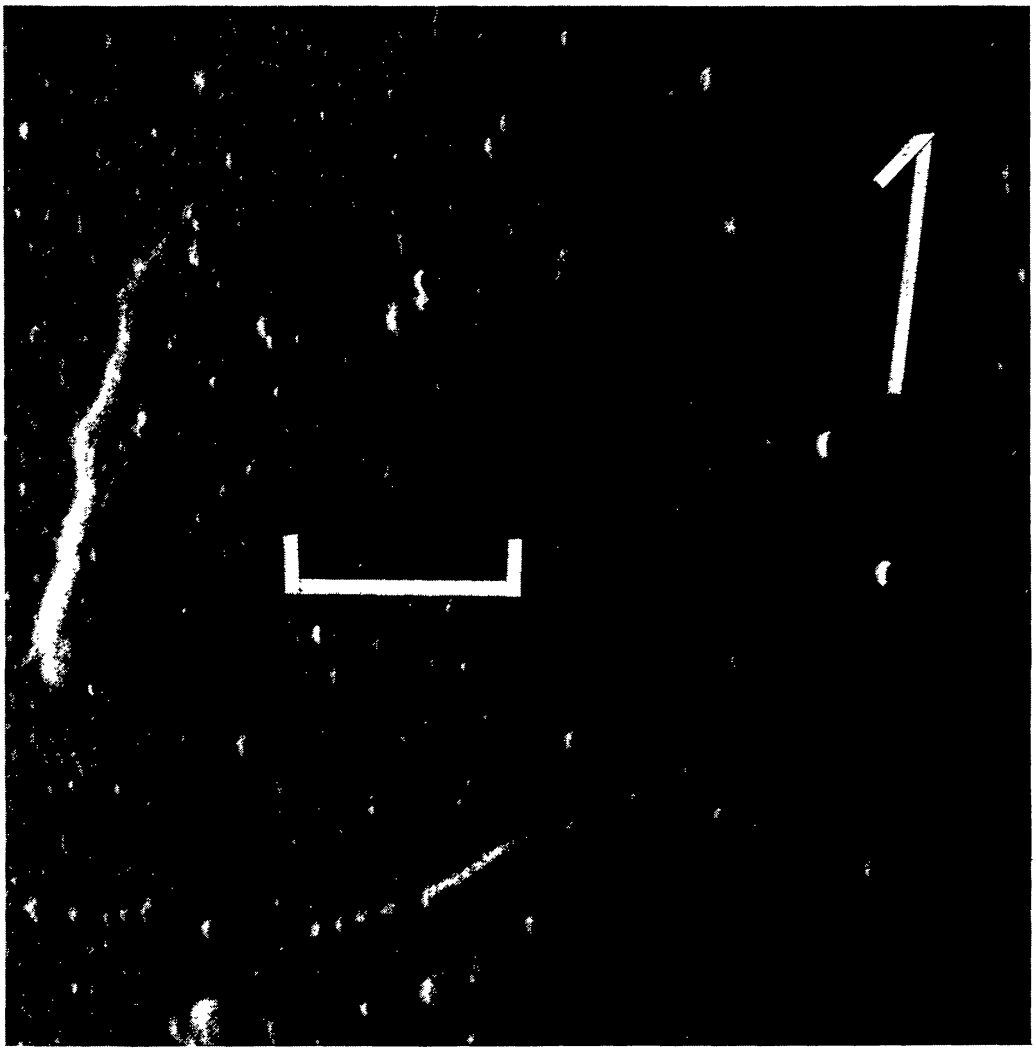

Fig. 3. Genetic type 2 crater chain in southeastern Mare Serenitatis (19.9°N, 27.5°E). The chain runs from upper left to lower right and consists of two conical cratered mounds with a line of rimless craters and small hummocks in between. Also note the group 1 crater chain extending across the upper edge of the photo. The scale bar is 5 km, and the arrow points north. NASA Photo AS17-2317.

a group 1 crater chain passes south of the chain, but direct relationship between these features is not seen. Both cones are relatively fresh, with no layering or structure visible in either the walls or rim. The chain is 14.4 km long. The northern cone is 1.4 km wide at the base, and the rim is approximately 150 m high. The southern cone is 1.9 km wide and the rim is approximately 120 m high. The slope on the northern cone is approximately 12° and the slope on the southern cone is approximately 8°.

Extensive studies of cinder cone growth in different planetary environments have been conducted by McGetchin and Head (1973) and by McGetchin *et al.* (1974), using Northeast Crater, Mount Etna, Sicily, as an example of a terrestrial cinder cone. These authors have determined that the form of the cinder cone will be determined by eruption velocity and launch angle, volume of the ash erupted,

and gravity and atmospheric conditions. McGetchin and Head (1973) show that for an idealized lunar cinder cone of volume 3×10^6 m^3 and eruption conditions similar to Northeast Crater, the cone rim will be 209 m from the vent with a maximum height of 3 m, a width of 100–330 m, and a maximum slope of 1.3°. The limit of continuous ejecta will be at 1500 m. As reported by McGetchin *et al.* (1974), an eruption less vigorous than Northeast Crater would concentrate pyroclastic ejecta closer to the vent, resulting in a higher rim, smaller radius of continuous ejecta, and a higher average maximum slope. More vigorous eruption conditions would have the opposite effect, dispersing ejecta and resulting in a lower rim, larger radius of continuous ejecta, and a lower average maximum slope. The cinder cones in the Mare Serenitatis crater chain described above appear to be much higher, with steeper slopes than the idealized cone of McGetchin and Head (1973), indicating less violent eruption conditions for this chain. This conclusion was also reached by Scott (1974).

The presence of possible pyroclastic ejecta in soil samples returned on Apollos 11, 15, and 17 supports the possibility of lunar cinder cones. Dark-mantle material sampled at the Apollo 17 landing site consists of orange and black glass droplets which are exceptionally well sorted, petrographically and chemically homogeneous, and have complicated surface morphologies which may indicate formation in a fire fountain (Heiken *et al.*, 1974). The shape of individual droplets ranges from simple spheres to composite forms which are covered with smaller droplets of the same composition. The surface of individual droplets often have small, low-velocity impact spalls.

The black spheres are primarily composite forms which appear to be more completely recrystallized orange droplets. Heiken *et al.* (1974) feel that pyroclastic origin for these soils is supported by the extreme chemical and petrographic homogeneity which would not be expected in glass spheres of impact origin. The composite forms would arise from continued recycling of already formed droplets through a fire fountain which would account for the smaller spatter droplets on the composite forms and the low-velocity impact spalls. McKay *et al.* (1974) used a similar argument to account for surface features on the Apollo 15 green glass spheres.

The location of the Mare Serenitatis crater chain also supports the cinder cone hypothesis. The area was described by Bryan and Adams (1974) as showing evidence of internal activity in the form of graben and rille structures, wrinkle ridges, and subsidence lineaments. The crater chain also lies within a band of the Mare Serenitatis dark-mantle material which has been interpreted as being of pyroclastic origin (Adams *et al.*, 1974).

General Features of Highland Crater Chains

Crater chains located in the lunar highlands range from 1 to 113 km long, with a mean length of 34 km. The degraded state of most highland crater chains makes determination of origin impossible on 27 of the 30 chains identified. The remaining three chains are in group 3. Crater degradation was within categories 3–4.5 of

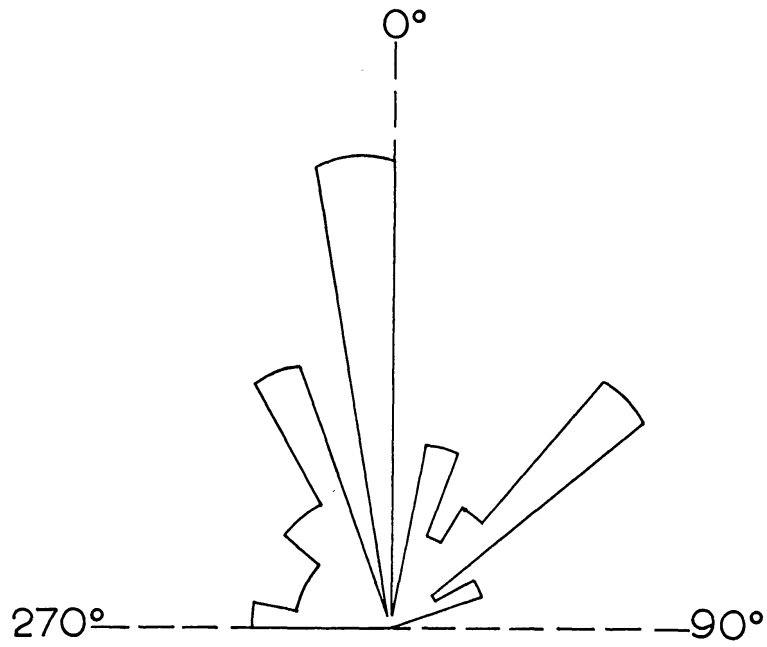

Fig. 4. Pie diagram of the axial trends of highland crater chains. Measurement interval is 10°. Total of 30 measurements.

Pohn and Offield (1970). A plot of axial trends of highland crater chains (Fig. 4) reveals much stronger evidence of structural control, apparently determined in part by the lunar grid system at 330° and 45°. Although the number of data points is higher than for mare crater chains, the same reservations apply for interpreting the data.

Group 3: *Possible highland volcanoes*

The chain is located on the floor on Mendeleev Crater (141.0°E, 7.0°N) and consists of 25 low rimmed craters arranged in a dumbbell pattern with large craters at either end and small craters in between (Fig. 5). Craters are bowl-shaped to conical, the variation probably caused by mass-wasting. There is an offset in the chain of 3.6 km near the southern end. This might be due to faulting or inhomogeneities in the crater floor deposits. No blocks or structure are visible in the crater walls possibly due to the masking effects of regolith. The trend of the chain may indicate that it has formed on a linear weakness in the crust which preceded the formation of Mendeleev Crater. The linear trend, symmetrical dumbbell shape, and the lack of relationship with any known feature produced by impact cratering indicates a possible endogenetic origin for the chain. The results of a detailed study of the Mendeleev Crater chain can be found in Eppler and Heiken (1974).

Direct comparison of highland crater chains to terrestrial features is difficult because of the degraded state of these features. Primary evidence for endogenetic origin is the alignment of these features with moon-wide structural trends associated with the lunar grid system (Fielder, 1961). As shown previously, a plot

1975LPSC....6.2571E

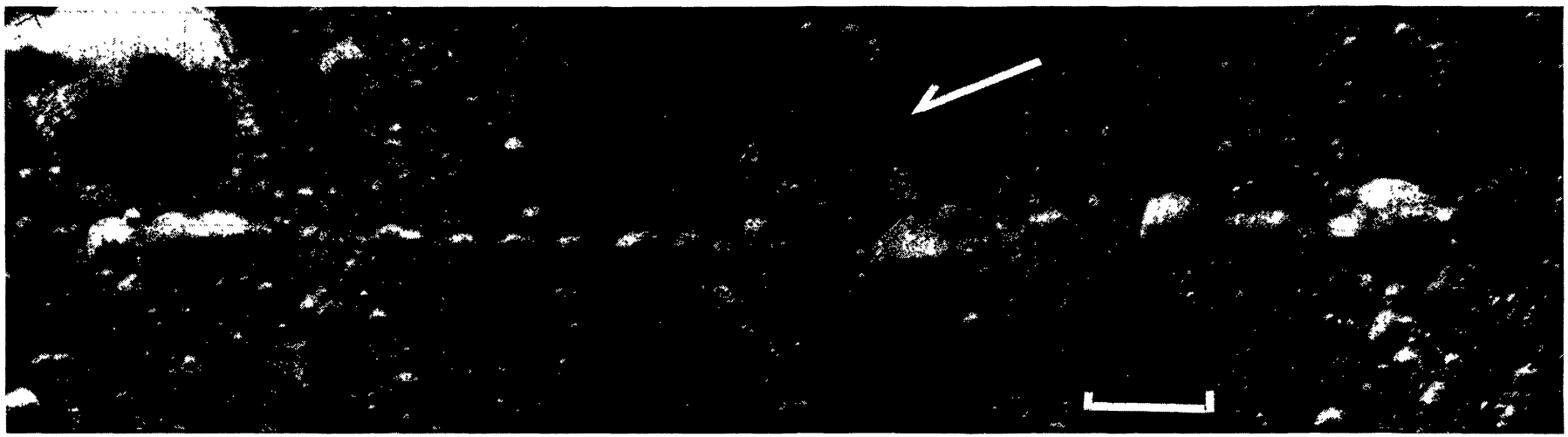

Fig. 5. Genetic type 3 on the floor of Mendeleev Crater (5.7°N, 138.8°E). The scale bar is 10 km, and the arrow points north. NASA Photo AS16-0345.

of highland volcanic crater chains shows possible preferential alignment of 330°, 360°, and 45°. These chains are apparently not related to any major impacts which occurred after the formation of the mare basins. Relative age relationships between the group 3 Mendeleev Crater chain and the floor of Mendeleev Crater indicate that the crater chain is much younger than the Cayley Formation crater floor material and is probably not the result of ejecta from a basin forming impact. These crater chains also lack any evidence of the geomorphic features associated with secondary impact crater chains.

Age of Apollo samples from the lunar highlands indicate an apparent lack of major volcanic events in the lunar highlands after approximately 4.3 AE (Tera *et al.*, 1973). However these crater chains may represent isolated volcanic events triggered by tectonic activity or nearby meteorite impacts.

In an attempt to determine the morphology of highland volcanoes, theoretical viscosities were calculated using the method of Shaw (1971) for lunar samples having compositions inferred from orbital X-ray data to be similar to rocks on the floor of Mendeleev crater. Adler *et al.* (1972) reported Al/Si concentration ratios of 0.71 for the Mendeleev Crater region, 0.67 for sample 15418, and 0.82 for sample 12037, 1151. The calculated theoretical viscosities at 1000°C are 2×10^4 poise for 15418 and 5.8×10^3 poise at 1070°C for basalt flows from Mauna Loa, Hawaii. This may infer that the properties of lava or tephra from the Mendeleev Crater chain was similar to terrestrial basaltic lavas. Consequently, the original form of highland crater chains may have been similar to crater chains produced by lunar basaltic volcanism; e.g. crater chains of groups 1 and 2.

Discussion and Conclusions

The origin of mare crater chains by collapse of lava tubes or through the formation of cinder cones is consistent with the currently accepted views of mare basin evolution. Astronaut photographs of the west wall of Hadley Rille imply that the mare basins were filled by a succession of thin flows. Work by Schaber (1973) and Brett (1974) supports this implication. Based on investigations of terrestrial lava flows, it is expected that numerous lava tubes would form during the filling of a mare basin.

Spectral reflectance studies of the distribution of dark-mantle deposits by Adams *et al.* (1974) indicate a widespread distribution for these pyroclastic materials on the near side of the mood. This may imply that volcanic fire fountains were fairly common during episodes of mare fill, and numerous cinder cone complexes may have been built during a single eruption cycle. For example, Schaber (1973) reported a low-albedo cinder cone complex at the southeast end of Euler β which may be genetically and structurally related to the source of phase III Eratosthenian lava flows.

The primary evidence for highland volcanic crater chains is their alignment with moon-wide structural trends and their lack of genetic or morphologic relationship with known impact craters. Although results from the Apollo 16 mission raised doubts as to the existence of highland volcanic activity younger

than 4.3 AE, and the areal distribution of group 3 crater chains appears to be limited, the authors suggest that further study of Apollo and Orbiter photographs may indicate a larger distribution of these events.

From the results of the study, the following conclusions can be drawn:

(1) Mare crater chains may be either collapsed lava tubes or lines of cinder cones. Either or both of these possibilities is consistent with current concepts of mare basin evolution, and with investigations of possible pyroclastic ejecta in returned soil samples from Apollos 11, 15 and 17.

(2) Theoretical viscosities calculated for returned samples with Al/Si concentration ratios similar to the floor of Mendeleev Crater are analogous to measured viscosities of some terrestrial basalt flows. This may infer that the manner of formation and the original morphology of highland crater chains may have been similar to crater chains produced by basaltic volcanism, e.g. mare crater chains.

(3) A plot of the axial trends of mare crater chains does not reveal any significant structural trends for these chains. Highland crater chains, however, appear to be oriented in part along the lunar grid system at 45°, 330°, and 360°. From these data we infer that highland volcanism may occur along linear weaknesses in the original lunar crust.

Acknowledgments—The authors wish to thank the staff of the Lunar Science Institute for technical assistance, T. Bornhorst for providing and running the computer program which calculated the theoretical viscosities used in the paper and S. Hamilton for typing the final manuscript. This paper benefited greatly from discussions with W. Elston, F. Hörz, D. Kinsler, and M. Prinz, and from critical reviews by J. M. Erickson, T. R. McGetchin, J. Street, and E. A. Whitaker. Eppler was supported by the Lunar Science Institute as a Visiting Graduate Fellow, by Lockheed Electronics Corporation, Houston, Texas, and by NASA grant NSG-7066 at the University of New Mexico. This paper is L.S.I. contribution 218.

REFERENCES

Adams J. B., Pieters C., and McCord T. B. (1974) Orange glass: Evidence for regional deposits of pyroclastic origin on the moon. *Proc. Lunar Science Conf. 5th*, p. 171–186.

Adler I., Trombka J., Gerard J., Lowman P., Schmadebeck R., Blodget H., Eller E., Yin L., Lamonte R., Osswald G., Gorenstein P., Gursky H., Harris B., Golub L., and Harden F. R. (1973) X-ray fluorescence experiment. In *Apollo 16 Preliminary Sci. Report*, NASA publication SP-315, p. 19-1 to 19-14.

Brett R. (1974) Thickness of some lunar mare basalt flows and ejecta blankets based on chemical kinetic data. *Geochim. Cosmochim. Acta.* In press.

Bryan W. B. and Adams M. L. (1974) Some volcanic and structural features of Mare Serenitatis. In *Apollo 17 Preliminary Sci. Report*, NASA publication SP-330, p. 30-9 to 30-13.

Cruikshank D. P. and Wood C. A. (1972) Lunar rilles and Hawaiian volcanic features: Possible analogues. *The Moon* **3**, 412–447.

El-Baz F. (1969) Crater characteristics. In *Analysis of Apollo 8 Photograph and Visual Observations*, NASA publication SP-201, p. 25-29.

Elston W. E., Laughlin A. W., and Brower J. A. (1971) Lunar nearside tectonic patterns from Orbiter 4 photographs. *J. Geophys. Res.* **76**, 5607–5682.

Eppler D. B. and Heiken G. H. (1974) The Mendeleev Crater chain: A description and discussion of origin. *NASA TM X-58108*, Johnson Space Center, Houston. 12 pp.

Fielder G. H. (1968) Linear arrays of craters on the Ranger photographs. *Planet. Space Sci.* **16**, 501–508.

Fielder G. H. (1961) *Structure of the Moon's Surface.* Pergamon Press, New York.

Fielder G. H. and Marcus A. (1967) Further tests for the randomness of craters. *Monthly Notices Roy. Astron. Soc.* **136**, 1–10.

Greeley R. A. (1971a) Lava tubes and channels in the lunar Marius Hills. *The Moon* **3**, 289–314.

Greeley R. A. (1971b) Observations of actively forming lava tubes and associated structures. *NASA TM X-62014.* Johnson Space Center, Houston. 33 pp.

Greeley R. A. and Hyde J. (1972) Lava tubes of the cave basalt, Mt. St. Helens, Washington. *Geol. Soc. America Bull.* **83**, 2397–2418.

Guest J. E. and Murray J. B. (1971) A large scale surface pattern associated with the ejecta blanket and rays of Copernicus. *The Moon* **3**, 326–336.

Heiken G. H., McKay D. S., and Brown R. W. (1974) Lunar deposits of possible pyroclastic origin. *Geochim. Cosmochim. Acta.* **38**, 1703–1718.

Howard K. A., Head J. W., and Swann G. A. (1972) Geology of Hadley Rille. *Proc. Lunar Sci. Conf. 3rd*, p. 1–14.

MacDonald G. A. (1954) Activity of Hawaiian Volcanoes during the years 1940–1950. *Bull. Volcanologique* **15**, 119–179.

McGetchin T. R. and Head J. W. (1972) Lunar cinder cones. *Science* **180**, 168.

McGetchin T. R., Settle M., and Chouet B. A. (1974) Cinder cone growth modeled after Northeast Crater, Mt. Etna, Sicily. *J. Geophys. Res.* **79**, 3257–3272.

McKay D. S., Clanton U. S., and Ladle G. (1973) Scanning Electron Microscope study of the Apollo 15 green glass. *Proc. Lunar Sci. Conf. 4th*, p. 225–238.

Mutch T. A. (1971) *Geology of the Moon.* Princeton University Press. Princeton, N. J. 391 pp.

Oberbeck V. R. (1971) A mechanism for the production of lunar crater rays. *The Moon* **2**, 263–278.

Oberbeck V. R. and Morrison R. H. (1973) On the Formation of Lunar Herringbone Pattern. *Proc. Lunar Sci. Conf. 4th*, p. 107–124.

Ollier C. D. and Brown M. C. (1965) Lava Caves of Victoria. *Bull. Volcanologique* **28**, 215–229.

Pohn H. A. and Offield T. W. (1970) Lunar crater morphology and relative age determination of lunar geologic units. U.S. Geol. Survey Prof. Paper 700-C, p. C153–C169.

Schaber G. G. (1973) Lava flows in Mare Imbrium: Geologic evaluation from orbital photography. *Proc. Lunar Sci. Conf. 4th*, p. 73–92.

Schumm S. A. (1970) Experimental Studies on the Formation of Lunar Surface Features by Fluidization. *Geol. Soc. America Bull.* **81**, 2539–2552.

Scott D. H. (1974) Mare Serenitatis cinder cones and terrestrial analogs. In *Apollo 17 Preliminary Sci. Report*, NASA publication SP-330, p. 30-7 to 30-8.

Scott D. H., West M. N., Lucchitta B. K., and McCauley J. F. (1972) Preliminary geologic results from orbital photography. In *Apollo 14 Preliminary Sci. Report*, NASA publication SP-272, p. 274–283.

Shaw H. R. (1972) Viscosities of magmatic silicate liquids: An empirical method of prediction. *Amer. J. Sci.* **272**, 870–893.

Shemyakin M. M. (1969) Peculiarities in the dispositions and dimensions of craters in lunar crater chains. *Sol. Syst. Res.* **3**, 53–60.

Shoemaker E. M. (1962) Interpretation of Lunar Craters. In *Physics and Astronomy of the Moon* (editor Z. Kopal), p. 283–360.

Tera F., Papanastissiou D., and Wasserberg G. J. (1973) A lunar cataclysm at 3.95 AE and the structure of the lunar crust (abstract). In *Lunar Science IV*, p. 723–726. The Lunar Science Institute, Houston.